Publication I

R. C. D. Paiva, J. Pakarinen, and V. Välimäki. Acoustics and modeling of pickups. *J. Audio Engineering Society*, vol. 60, no. 10, pp. 768–782, Oct. 2012.

Acoustics and Modeling of Pickups

RAFAEL C. D. PAIVA,[1,2] *AES Member,* **JYRI PAKARINEN,**[1] *AES Member,* **AND**
(rafael.dias.de.paiva@aalto.fi) (jyri.pakarinen@gmail.com)

VESA VÄLIMÄKI,[1] *AES Fellow*
(vesa.valimaki@aalto.fi)

[1]*Department of Signal Processing and Acoustics, Aalto University, Espoo, Finland*
[2]*Nokia Institute of Technology, INdT, Brasilia, Brazil*

An electromagnetic pickup capturing vibrations of steel strings in electric stringed instruments modifies the timbre of the instrument in various ways. The acoustic characteristics and modeling of the pickup position, the sensitivity width of the pickup, the dispersion of waves in a steel string, mixing options of several pickups, linear resonant filtering of the pickup circuit itself, and the distortion caused by the distance-dependent magnetic flux are studied.

0 INTRODUCTION

Pickups comprise an important part of the timbre of certain string instruments. Guitar players recognize their importance, and incorporate each type of pickup, as well as their position, together with the microphone positioning placement [1], to a specific style or timbre. For example, some guitar players prefer humbucker pickups [2] located at the bridge for playing with distortion, but single coils at middle and neck positions for a cleaner timbre. Additionally, other instruments, such as the Clavinet [3], use this kind of device for capturing the vibrations of a string.

Pickup models comprise one class of effects obtained with virtual analog modeling [4], which is currently an active research topic in audio signal processing. It includes emulation of guitar distortion circuits and amplifiers [5, 6, 7, 8] and analog reverberators [9, 10], among others.

A magnetic pickup is a device used to capture the string vibration on steel stringed musical instruments [11]. It is built using a permanent magnet with a winding around it, and it captures the string vibration through the magnetic variation caused by the proximity of the strings. Since the strings are, in this case, built using a high permeance material, they offer a favorable path for the magnetic flux. Hence, the magnetic flux is larger when the string is closer to the magnet than when further.

The first effect of pickups reported in the literature is related to the position where they are placed. The pickup placement produces a comb filter effect, which enhances certain frequencies while attenuating others [11]. This explains why bridge pickups yield a brighter sound than middle and neck pickups. This behavior can be understood, and a pickup position model can be obtained by evaluating a waveguide string model [12, 13, 14, 15]. This kind of model is often used in synthesis [16, 17, 18, 19] and in commercial products [20, 21]. As well as the position of the pickups, instruments often offer the possibility of mixing pickups at different positions. The phase differences between responses at different positions make this kind of combination to have a complex frequency response, which could enhance, or even attenuate, certain frequency bands [22].

In addition to the position of pickups, the way they are built offers different timbres among different manufacturers and models. Most of this characteristic timbre is explained by the equivalent circuit, which often presents a prominent resonance [11]. Additionally, the frequency of this resonance is highly variable among different models, which also depends on the number of turns used in the winding as well as on the material used in the core and for the wire's insulation [23, 24].

Finally, the mapping between the string movement and the magnetic flux captured by the pickup is nonlinear and is different when the polarization of the string movement changes. Models for this behavior are obtained from integral equations representing the magnetic flux at the string and how it changes the magnetic flux at a measurement position [25, 26].

An overview of the elements affecting the pickup timbre is shown in Fig. 1. First there are the effects of the pickup position and the sensitivity width, which are a comb filter and a low-pass filter. At this stage, the calculated value is

Manuscript received 2010 December 13; revised 2011 November 11.

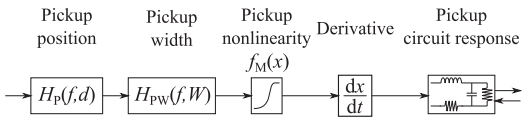

Fig. 1. Overview of pickup elements.

equivalent to the sensed string position above the pickup, and a nonlinear function maps this position to the magnetic flux in the pickup. The magnetic flux is related to the pickup output voltage by a derivative operation, and the final output voltage is the result of filtering this signal with a resonant filter formed by the pickup equivalent circuit impedance. A digital implementation of the proposed pickup model can be used in electric guitar synthesis [13, 27, 28, 29] and effects processing.

This work presents an overview of the techniques and modeling issues related to magnetic pickups with some new developments. Section 1 presents a mathematical foundation for determining the effect different positions have over the guitar timbre, while Sections 2 and 3 use the same framework for determining new models for the effects of mixing options of one or more pickup signals and different sensitivity widths, respectively. In Section 4 an extension to the model related to the pickup position presented in Section 1 is analyzed, considering the dispersive propagation of waves in a steel string. The circuit elements related to the pickups are analyzed in Section 5, where a new model for the circuit impedance is derived and a new analysis for the combination of pickups is presented. In Section 6, a new analysis using a finite element model reveals the nonlinear mapping between magnetic flux and the string position. Conclusions are presented in Section 7.

1 PICKUP POSITION

The position of magnetic pickups plays a major part in the guitar timbre and is an important parameter used by guitar players. Pickups placed next to the bridge yield a bright tone, while a darker tone is achieved when the pickup distance to the bridge is increased. Hence, guitars often have two or three pickups, as shown in Fig. 2. For example, Les Paul-type guitars traditionally have two humbucker pickups, one at the bridge and the other at the neck, whereas Stratocaster guitars traditionally have three pickups: bridge, middle, and neck. This effect is related to how the waves propagate through a string and the standing waves that are generated by this behavior.

A simple approach to determine the pickup position effect is based on analyzing the standing waves on a string [30, 31]. Fig. 3 shows the standing waves composed of four harmonics in a string and the possible placement of two pickups P1 and P2. Notice that when the open string in Fig. 3(a) is played, P2 has higher energy in the first and second harmonics than P1, while the fourth harmonic is almost not sensed. When the string in Fig. 3(b) is pressed at a different position, P2 senses more energy in the first harmonic than P1, but the third harmonic is suppressed in

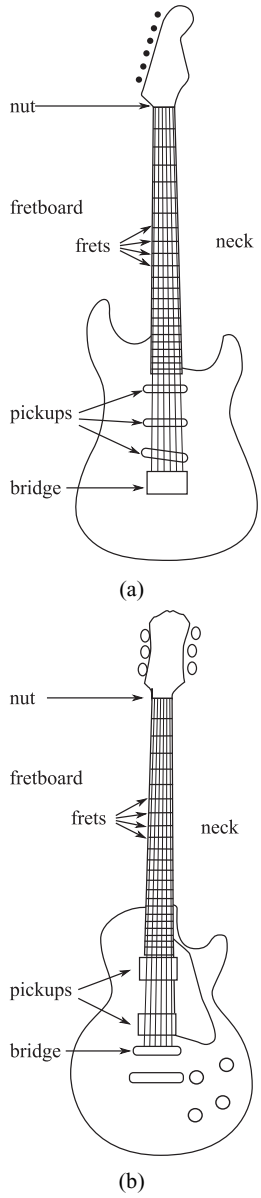

Fig. 2. Typical position of pickups in electric guitars in (a) a Stratocaster model and (b) a Les Paul model.

turn. For the second and fourth harmonics, similar energy is transferred to P1 and P2.

Considering a string of length L and a pickup positioned at d, the pickup frequency response $H_P(f, d)$ may be obtained as

$$H_P(f, d) = \sin\left(\frac{\pi d f}{L f_0}\right), \tag{1}$$

where f is the analysis frequency and f_0 is the first harmonic frequency of the open guitar string [31]. Although

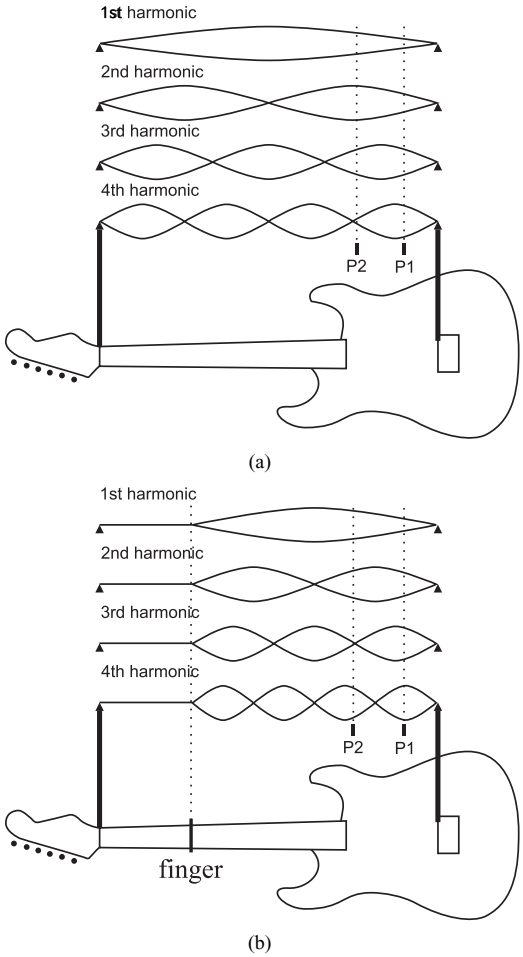

Fig. 3. Pickup position effect based on standing waves (adapted from [30, 31]).

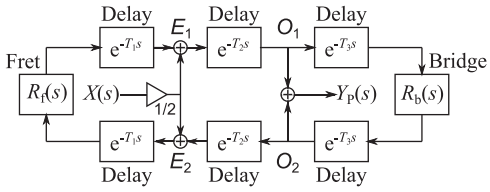

Fig. 4. General delay-line-based string model for plucking point and pickup position evaluation, adapted from [14].

this approach is capable of defining the pickup response given by its position, it fails to determine other important factors, such as imperfect reflection coefficients at string terminations.

A framework for analyzing the effect of the pickup position is shown in Fig. 4, where a waveguide model for a string is presented in the continuous-time Laplace domain [12]. In the model of Fig. 4, the transfer functions $R_f(s)$ and $R_b(s)$ represent the reflection from the fret and the bridge, respectively, s is the complex frequency variable of the Laplace transform, the terms $e^{-s\tau}$ represent delays of τ seconds in the Laplace domain, $X(s)$ represents an excitation signal at the plucking point, and $Y_P(s)$ represents the output signal at the pickup. This model uses two traveling waves propagating in opposite directions with a total delay of $2T_0 = 2(T_1 + T_2 + T_3)$ seconds.

The fundamental frequency of the string f_0 is related to the total time delay T_0 by

$$f_0 = \frac{1}{2T_0}, \tag{2}$$

and the delay times are related to the time a wave takes to propagate from the fret to the plucking point T_1, from the plucking point to the pickup point T_2, and from the pickup point to the bridge T_3. Hence, the string displacement above the pickup can be determined as [14]

$$Y_P(s) = O_1(s) + O_2(s) = O_1(s)\left[1 + H_{O1O2}(s)\right], \tag{3}$$

where $O_1(s)$ and $O_2(s)$ are the traveling waves at the pickup point in the Laplace domain, and

$$H_{O1O2}(s) = R_b(s)e^{-2T_3 s} \tag{4}$$

is the transfer function between the observation points O_1 and O_2. The incoming wave at the pickup point $O_1(s)$ can be rewritten as

$$\begin{aligned} O_1(s) &= \tfrac{1}{2}X(s)\left[1 + H_{E2E1}(s)\right]H_{E1O1}(s) \\ &\quad + O_1(s)H_L(s) \\ &= \tfrac{1}{2}X(s)H_{E1O1}(s)\tfrac{1+H_{E2E1}(s)}{1-H_L(s)}, \end{aligned} \tag{5}$$

where $H_{E2E1}(s)$ is the transfer function between the excitation points E_1 and E_2, $H_{E1O1}(s)$ is the transfer function between the excitation point E_1 and the observation point O_1, and

$$H_L(s) = R_b(s)R_f(s)e^{-2T_0 s} \tag{6}$$

is the transfer function of the feedback loop. Thus, the final output regarding the pickup position is

$$Y_P(s) = \frac{1}{2}X(s)H_P(s)\frac{1 + H_{E2E1}(s)}{1 - H_L(s)}, \tag{7}$$

where the pickup effect $H_P(s)$ is given by

$$H_P(s) = \left[1 + H_{O1O2}(s)\right]H_{E1O1}(s). \tag{8}$$

Since the reflection transfer function at the bridge is often approximated by a constant $R_b(s) = -\beta$, where $0 < \beta < 1$, and the term $H_{E1O1}(s)$ stands for a constant delay that can be ignored in this analysis, the pickup position effect can be approximated by

$$H_P(s) = 1 - \beta e^{-2T_3 s}, \tag{9}$$

where the squared magnitude of the frequency response is obtained replacing s by $j\omega$ in Eq. (9):

$$\begin{aligned} |H_P(\omega)|^2 &= \left(1 - \beta e^{-2T_3 j\omega}\right)\left(1 - \beta e^{2T_3 j\omega}\right) \\ &= 1 - 2\beta\cos(2\omega T_3) + \beta^2, \end{aligned} \tag{10}$$

where ω represents the analysis frequency in rad/s and $j = \sqrt{-1}$ is the imaginary unit. Hence, the pickup position

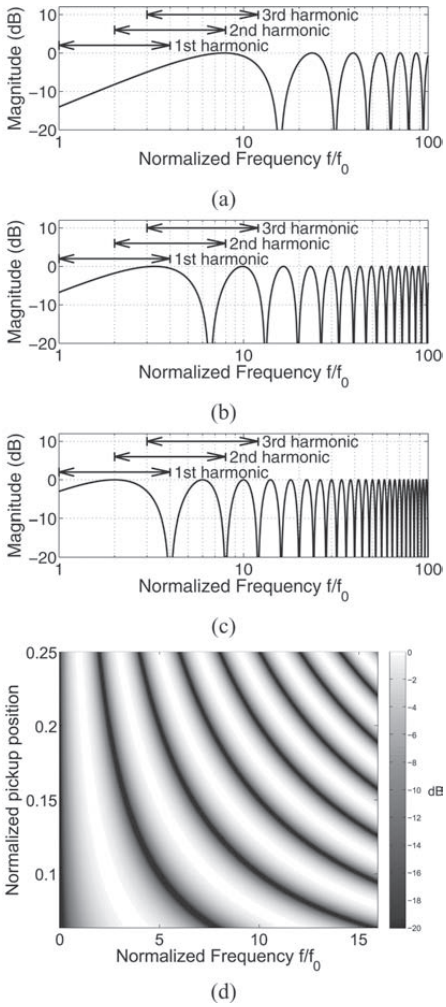

Fig. 5. Effect of pickup position for a pickup positioned at the (a) bridge, (b) middle, and (c) neck positions, and (d) an image showing the response for intermediate positions.

effect is given by a minimum value in $|H_{\mathrm{P}}(\omega_m)| = 1 - \beta$ at harmonic frequencies $\omega_m = \frac{\pi k}{T_3}$, with $k = 0, 1, \ldots$, and a maximum value $|H_{\mathrm{P}}(\omega_M)| = 1 + \beta$ at $\omega_M = \frac{\pi(k+0.5)}{T_3}$, with $k = 0, 1, \ldots$.

Typical pickup positions in a Stratocaster guitar are the bridge, middle, and neck positions located at 4.1 cm, 9.8 cm, and 16.2 cm from the bridge, respectively, for a string of 64.8 cm [31]. For these positions different magnitude responses will be observed, which are shown in Fig. 5 for a normalized frequency f/f_0, where f_0 is the fundamental frequency of the open string and $\beta = 1$. In Fig. 5, horizontal arrows are drawn to visualize the location of the first, second, and third harmonics for the 24 frets of the guitar.

The pickup response at the bridge is shown in Fig. 5(a), where the fundamental frequency is seen to be attenuated for most of the notes, as there is a 14-dB and a 7-dB attenuation at f_0 and $2f_0$, respectively. Additionally, the second and third harmonics have their amplitudes increased in relation to the first harmonic for a large fundamental frequency. This results in a bright perceived sound at the bridge pickup. The middle pickup response, shown in Fig. 5(b), has a lower attenuation for the first harmonic. For most of the fret positions, the second harmonic is enhanced since the main lobe of the frequency response has a maximum between about $2f_0$ and $5f_0$, while the third harmonic has its amplitude decreased for high pitches with more than 5 dB attenuation when the fundamental frequency lies between $1.6f_0$ and $2.6f_0$. This leads to a darker response for the middle pickup when compared to the bridge pickup. The neck pickup response, shown in Fig. 5(c), on the other hand presents a pronounced first harmonic. Now, the second and third harmonics vary between this pickup's responses' maximum and minimum depending on the fundamental frequency. Hence the neck pickup has the darkest response.

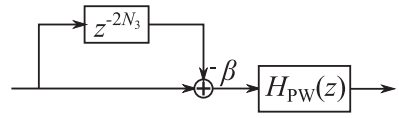

Fig. 6. Comb filter implementation for pickup position and width modeling using the filter $H_{\mathrm{PW}}(z)$.

The pickup position effect may be approximated in a discrete-time model by taking the impulse-invariant transform of Eq. (9)

$$H_{\mathrm{P}}(z) = 1 - \beta z^{-2N_3}, \tag{11}$$

where z^{-1} represents the unit delay in the z transform domain; $N_3 = \mathrm{round}(T_3 f_{\mathrm{s}})$ is the equivalent discrete time delay in samples, to approximate a delay of T_3 seconds, which is proportional to the pickup distance to the bridge; and f_{s} is the sampling frequency. The implementation of the comb filter described by Eq. (11) is presented in Fig. 6, which includes a delay line of length $2N_3$ samples and the reflection coefficient β [14]. Cascaded with this position model is $H_{\mathrm{PW}}(z)$, which is discussed in Section 3. This model can be further improved by using a fractional delay filter to approximate the delay of $T_3 f_{\mathrm{s}}$ samples instead of using an integer sampling period delay [32].

2 PICKUP MIXING EFFECT

In addition to choosing the pickup position, most electric guitars offer the possibility of mixing pickup signals. Since the pickups capture traveling waves in the string at different positions, they have different delays relative to each other. Hence, by combining the signals of two pickups the phase differences may boost or attenuate certain frequencies [22].

In order to determine the mixing effect, the pickup response with the total delay needs to be considered as in Eq. (8), whose Fourier transform is given by

$$\begin{aligned} H_{\mathrm{P}}(\omega) &= \left(1 - \beta \mathrm{e}^{-2T_3 \mathrm{j}\omega}\right) \mathrm{e}^{-(T_0 - T_1 - T_3)\mathrm{j}\omega} \\ &= \left(1 - \beta \mathrm{e}^{-2T_3 \mathrm{j}\omega}\right) \mathrm{e}^{T_3 \mathrm{j}\omega} \mathrm{e}^{-(T_0 - T_1)\mathrm{j}\omega}, \end{aligned} \tag{12}$$

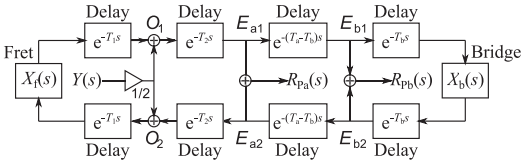

Fig. 7. General delay-line-based string model for pickup mixing evaluation.

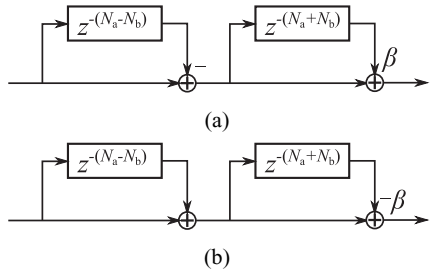

Fig. 8. Comb filter implementation for equal pickup mixing for (a) in-phase and (b) out-of-phase configurations.

which can be simplified into the following non-causal model, ignoring the linear delay element $e^{-(T_0-T_1)j\omega}$:

$$H_P(\omega) = e^{T_3 j\omega} - \beta e^{-T_3 j\omega}. \tag{13}$$

If the same pickups with the same circuit response are assumed to be used, the joint response can be determined as the sum of both responses $H_P(\omega)$ with different pickup-to-bridge delays T_3. For two pickups with frequency responses given by $H_{Pa}(\omega)$ and $H_{Pb}(\omega)$ whose signals are mixed in-phase, the response is determined as

$$\begin{aligned} H_{Pa+b}(\omega) &= H_{Pa}(\omega) + H_{Pb}(\omega) \\ &= e^{T_a j\omega} - \beta e^{-T_a j\omega} + e^{T_b j\omega} - \beta e^{-T_b j\omega} \\ &= 2\left(e^{\frac{T_a+T_b}{2} j\omega} - \beta e^{-\frac{T_a+T_b}{2} j\omega}\right) \\ &\quad \cos\left(\tfrac{T_a-T_b}{2}\omega\right), \end{aligned} \tag{14}$$

where T_a and T_b are the delays between pickups a and b and the bridge, as shown in Fig. 7. For $\beta = 1$, Eq. (14) can be simplified as

$$H_{Pa+b}(\omega) = 4j \sin\left(\frac{T_a + T_b}{2}\omega\right) \cos\left(\frac{T_a - T_b}{2}\omega\right). \tag{15}$$

A similar response is found when pickups in opposite phase are considered, given by

$$\begin{aligned} H_{Pa-b}(\omega) &= H_{Pa}(\omega) - H_{Pb}(\omega) \\ &= e^{T_a j\omega} - \beta e^{-T_a j\omega} - e^{T_b j\omega} + \beta e^{-T_b j\omega} \\ &= 2j\left(e^{\frac{T_a+T_b}{2} j\omega} + \beta e^{-\frac{T_a+T_b}{2} j\omega}\right) \\ &\quad \sin\left(\tfrac{T_a-T_b}{2}\omega\right), \end{aligned} \tag{16}$$

which can also be simplified, when perfect reflection ($\beta = 1$) is assumed, to

$$H_{Pa-b}(\omega) = 4j \cos\left(\frac{T_a + T_b}{2}\omega\right) \sin\left(\frac{T_a - T_b}{2}\omega\right). \tag{17}$$

It should be noted that although the in-phase wiring of the pickups is a far more commonly used option, the out-of-phase connection is sometimes used in order to produce a hollow nasal tone. Notice that the magnitude responses in Eqs. (15) and (17) depend on the average and differences of times T_a and T_b. In both cases, the response is modeled by two out-of-phase comb filters, whose lobes have widths $\frac{T_a+T_b}{2}$ or $\frac{T_a-T_b}{2}$.

A digital implementation for the pickup mixing effect is shown in Fig. 8. The digital model can be devised by using two comb filters, one representing the average pickup position and the other representing the position difference, as illustrated in Fig. 8. The differences for in-phase and out-of-phase configurations in Figs. 8(a) and (b) are only in the summation signs. In this digital implementation, the discrete delay times are given by $N_a = \text{round}(T_a f_s)$ and $N_b = \text{round}(T_b f_s)$. In order to avoid non-causal delay in Fig. 8, the relation between the pickups should be such that $N_a > N_b$. Again, this model can be improved by using fractional delay filters instead of an integer sampling period delay [32].

The responses for typical configurations in electric guitars are shown in Fig. 9. The in-phase configurations in Fig. 9(a), (c), and (e) show little attenuation for the first harmonic at the lowest octave. For the middle plus bridge configuration in Fig. 9(a), the second harmonic also fits mostly within the main lobe of the frequency response. In the bridge plus neck configuration in Fig. 9(e), the second harmonic is situated mostly at a notch in the frequency response.

All the responses for opposite phase configurations in Fig. 9(b), (d), and (f) show a large attenuation for the main lobe in the frequency response. This provides a strong attenuation of the fundamental frequency, which can also be easily visualized by analyzing the standing wave configurations of Fig. 3. Since the fundamental frequency standing wave is always in phase for different pickups, by mixing pickup signals out of phase the amplitude of first harmonic will be the difference between the amplitude at both pickups. The second harmonic is in all cases mostly in the second lobe of the frequency response, which is enhanced significantly in the neck minus bridge configuration in Fig. 9(f). In all cases, the higher frequencies are following complex patterns given by the combination of both comb filters.

3 PICKUP WIDTH EFFECT

In addition to the comb filter effect caused by different locations of the pickup, the sensitivity width also influences the pickup frequency response [31]. Pickup sensitivity can be understood in an intuitive way by observing Fig. 10, where the pickup is sensitive to an area of the string instead of to a single point, in which some vibration modes may change polarization. Hence, the width effect is expected to cause a low-pass filtering effect. The pickup sensitivity may be assumed to be given by the function $g_{PW}(x)$, where x represents the displacement about the pickup center P, and may be related to the framework given in Fig. 4 by

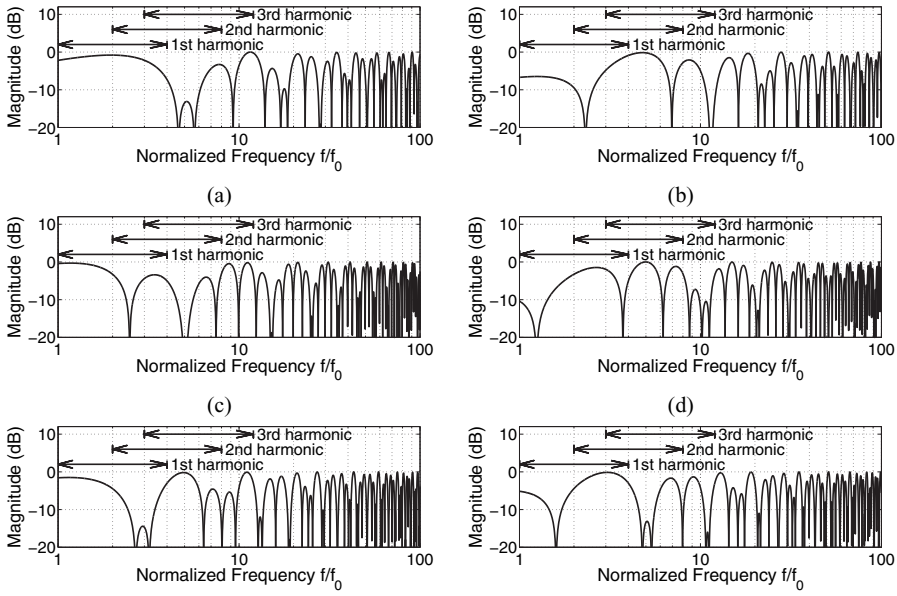

Fig. 9. Effect of mixing pickup signals at different positions for pickups at the (a) bridge and middle, (b) bridge and middle with opposite phases, (c) neck and middle, (d) neck and middle with opposite phases, (e) neck and bridge, (f) neck and bridge with opposite phases.

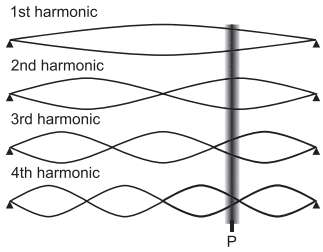

Fig. 10. Pickup width effect based on standing waves.

changing T_3 by its equivalent time delay $\tau = xT_0/L$, where L is the string length and $T_0 = 1/(2f_0)$.

The pickup response may thus be represented as a sum of the string time-domain output $y(t, p)$ at different infinitesimal pickup positions p around its sensitivity area $P - W/2 < p < P + W/2$, where W is the sensitivity width:

$$y_{\mathrm{PW}}(t) = \int_{-W/2}^{W/2} g_{\mathrm{PW}}(x) y(t, P - x)\mathrm{d}x. \tag{18}$$

In Fig. 4 it is possible to observe that $y(t, P - x) = o_1(t, P - x) + o_2(t, P - x)$, where $o_1(t, P)$ and $o_2(t, P)$ are the incoming and outgoing waves in the time domain at the observation point P. Moreover, when considering that the delay line in Fig. 4 is ideal, the observation position differences x are mapped into time delays τ, i.e.,

$$\begin{cases} o_1(t, P - x) = o_1(t + \tau, P) \\ o_2(t, P - x) = o_2(t - \tau, P) \end{cases}, \tau = \frac{xT_0}{L}. \tag{19}$$

Hence, by replacing the position sensitivity function by an equivalent time function $g_{\mathrm{PW}}(x) = h_{\mathrm{PW}}(\tau)$, Eq. (18) can be rewritten as

$$\begin{aligned} y_{\mathrm{PW}}(t) &= \int_{-W/2}^{W/2} g_{\mathrm{PW}}(x)\,(o_1(t, P - x) \\ &\quad + o_2(t, P - x))\,\mathrm{d}x \\ &= \int_{-T_{\mathrm{W}}/2}^{T_{\mathrm{W}}/2} h_{\mathrm{PW}}(\tau) o_1(t + \tau, P)\mathrm{d}\tau \\ &\quad + \int_{-T_{\mathrm{W}}/2}^{T_{\mathrm{W}}/2} h_{\mathrm{PW}}(\tau) o_2(t - \tau, P)\mathrm{d}\tau, \end{aligned} \tag{20}$$

where $T_{\mathrm{W}} = WT/L$ is the time spread given by the sensitivity width W. If the pickup sensitivity is considered to be symmetric around its center, $h_{\mathrm{PW}}(\tau) = h_{\mathrm{PW}}(-\tau)$, then

$$\begin{aligned} y_{\mathrm{PW}}(t) &= \int_{-T_{\mathrm{W}}/2}^{T_{\mathrm{W}}/2} h_{\mathrm{PW}}(\tau)\,(o_1(t + \tau, P) \\ &\quad + o_2(t + \tau, P))\,\mathrm{d}\tau \\ &= \int_{-T_{\mathrm{W}}/2}^{T_{\mathrm{W}}/2} h_{\mathrm{PW}}(\tau) y(t + \tau, P)\mathrm{d}\tau, \end{aligned} \tag{21}$$

which can be interpreted as the convolution between $h_{\mathrm{PW}}(t)$ and the time response of the pickup at a single point $y_{\mathrm{P}}(t) = y(t, P)$. By using the convolution theorem, Eq. (21) can be written in the Laplace domain as

$$Y_{\mathrm{PW}}(s) = H_{\mathrm{PW}}(s) Y_{\mathrm{P}}(s), \tag{22}$$

indicating that the sensitivity width has a linear filtering effect.

The pickup width response can be obtained by approximating the sensitivity function $g_{\mathrm{PW}}(x)$. A rectangular

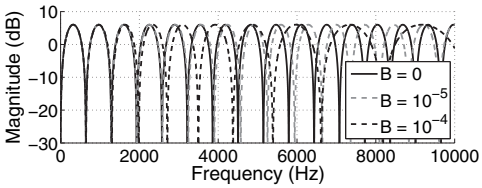

Fig. 11. Warped comb-filter responses caused by string dispersion.

window is indicated as an approximation in [31], but a Hamming or a truncated exponential window would probably be better modeling candidates, since the sensitivity is the highest at the center of the pickup. The sensitivity width response modeled by a Hamming window is given by

$$h_{\mathrm{PW}}(\tau) = a + (1-a)\cos\left(\frac{2\pi\tau}{T_{\mathrm{W}}}\right), \tag{23}$$

with $\frac{T_{\mathrm{W}}}{2} \leq \tau \leq -\frac{T_{\mathrm{W}}}{2}$. Thus, pickup sensitivity width results in a low-pass filtering effect, given by $H_{\mathrm{PW}}(\omega)$.

Implementation of a model for the pickup width is obtained by taking the z transform of Eq. (22):

$$Y_{\mathrm{PW}}(z) = H_{\mathrm{PW}}(z)Y_{\mathrm{P}}(z), \tag{24}$$

where $H_{\mathrm{PW}}(z)$ can be implemented with a discrete-time finite-impulse-response (FIR) filter approximating the continuous-time impulse-response $h_{\mathrm{PW}}(\tau)$. Fig. 6 shows how the width model would be implemented in cascade with the position model.

4 EFFECT OF STRING DISPERSION

In real strings, stiffness makes the wave speed frequency-dependent. Although this effect is small for high-pitched strings of guitars, it is important for the low-pitched strings [33]. This kind of effect is often responsible for the inharmonicity of strings [34], and will cause the notches in the pickup position response $H_{\mathrm{P}}(\omega)$ to be at inharmonic frequencies [29]. In this case, the delays represented in Fig. 4 and the phase delay of the string are modified by a correction factor given by (adapted from [35, 36])

$$\tau_\phi(\omega) = \frac{1}{\sqrt{1 + B\left(\frac{\omega}{\omega_0}\right)^2}}, \tag{25}$$

where ω_0 is the string fundamental frequency in radians per second and B is related to the inharmonicity constant [34].

When the total delay at a certain frequency is modified by the result in Eq. (25), the continuous-time Fourier transform for a delay operation is modified as

$$D(\omega, T_0) = \mathrm{e}^{-\mathrm{j}\omega T_0 \tau_\phi(\omega)}, \tag{26}$$

where T_0 represents the delay at $\omega = 0$. Hence, the comb filter that was derived in Eq. (10) is modified by the variable $\tau_\phi(\omega)$ as

$$|H_{\mathrm{P}}(\omega)|^2 = 1 - 2\beta\cos\left[2\omega T_3 \tau_\phi(\omega)\right] + \beta^2. \tag{27}$$

The effect derived in Eq. (27) is shown in Fig. 11, where an example of magnitude responses of comb-filters with

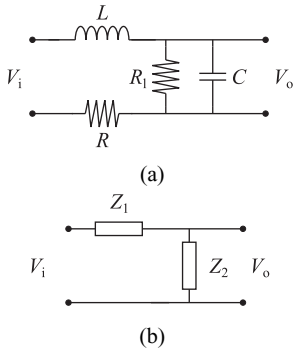

Fig. 12. (a) Pickup equivalent circuit, adapted from [23, 24]. (b) The equivalent circuit as a voltage divider.

typical values of B for low-pitched guitar strings are given [33]. This example is generated with $\beta = 1$, open string fundamental frequency $f_0 = 82$ Hz and $T_3 = 0.29$ ms, representing a bridge pickup located at 4.1 cm from the bridge for a string of 64.8 cm. As B is increased, the notches in the magnitude response are shown in Fig. 11 to deviate more from the ideal response with $B = 0$.

The implementation of a discrete-time model considering the dispersive string behavior can be obtained by using all-pass filters [37, 38, 35, 39]. In one approach, an all-pass filter is included after a delay line in order to distort the group delay to obtain the desired string inharmonicity [37, 38]. In this approach, a single all-pass filter may be used [35, 29] or a cascade of first-order filters [39] to model the desired string inharmonicity.

In another approach, a discrete-time model is obtained by substituting the delay units by all-pass filters implementing the dispersion [37, 38, 40]. One common structure of the all-pass filter which is used for frequency-warped signal processing is given by

$$\tilde{z}^{-1} = \frac{z^{-1} - a}{1 - az^{-1}}, \tag{28}$$

where a is the warping factor [41]. The all-pass filter in Eq. (28) has a phase delay given by

$$\tau_W(\hat{\omega}) = 1 + \frac{2}{\hat{\omega}}\arctan\left(\frac{a\sin(\hat{\omega})}{1 - a\cos(\hat{\omega})}\right), \tag{29}$$

where $\hat{\omega}$ represents the discrete-time angular frequency in radians per sample (adapted from [42, 43]). With a proper choice of the warping parameter a, it is possible to fit the phase delay to that caused by a given inharmonicity factor B.

5 PICKUP IMPEDANCE

Pickups are built with a permanent magnet to create the magnetic flux and a winding around it to transform the magnetic flux variations into voltage [11]. This can be designed in various ways, and alternative constructions can provide a modified pickup timbre. A pickup equivalent circuit is shown in Fig. 12(a), where V_{i} and V_{o} are the pickup circuit

input and output voltages, respectively [23, 24]. This circuit affects the pickup timbre, since the combination of the inductance L and capacitance C forms a resonant filter.

As any winding around a magnetic core, the pickup has an inductance L, whose value depends on the magnetic properties of the core and the number of turns of the winding. The winding is built using thin wires in order to increase the number of possible turns in the available space and increase the pickup inductance. The usual values for inductance are in the range $1\ \text{H} \leq L \leq 10\ \text{H}$ [23, 24]. Also, due to the high number of turns and the small thickness of wire, the pickup has a pronounced resistance accounting for ohmic losses. This is represented in the pickup model as a series resistance R in Fig. 12(a), whose typical values are in the range $5\ \text{k}\Omega \leq R \leq 15\ \text{k}\Omega$ [24].

Again, the small insulation separating the wire between each turn creates a parasitic capacitance. This capacitance per turn combines for a large number of turns forming C in Fig. 12(a). Although this capacitance is usually small, it creates a resonance with the inductance L in the audible range, which affects significantly the timbre of each pickup. Typical values for this capacitance are $15\ \text{pF} \leq C \leq 200\ \text{pF}$ [23, 24], and a minor variation in the pickup construction can significantly affect its value. Additionally, the capacitance of different circuits connected to the pickup output will affect its timbre.

Finally, the resistance R_l is used to represent the magnetic losses present in the permanent magnet. Its value is large, $300\ \text{k}\Omega \leq R \leq 3000\ \text{k}\Omega$ [24], and it influences the amplitude of the resonance peak caused by C and L.

The transfer function of the pickup due to the circuit elements $H_\text{c}(s)$ can be calculated by observing that the equivalent circuit in Fig. 12(a) is a voltage divider, as in Fig. 12(b). Hence [24]

$$\frac{V_\text{o}(s)}{V_\text{i}(s)} = H_\text{c}(s) = \frac{Z_2}{Z_1+Z_2} = \frac{1}{\left(1+\frac{R}{R_\text{l}}\right)+s\left(\frac{L}{R_\text{l}}+RC\right)+s^2LC}, \tag{30}$$

where a resonance will be observed around $\omega_\text{R} = 1/\sqrt{LC}$ [11]. Rewriting this equation to obtain the Fourier transform gives

$$H_\text{c}(\omega) = \frac{1}{\left(1+\frac{R}{R_\text{l}}\right)+\text{j}\omega\left(\frac{L}{R_\text{l}}+RC\right)-\omega^2LC}. \tag{31}$$

It should be observed that at low frequencies

$$\lim_{\omega\to 0} H_\text{c}(\omega) = \frac{1}{\left(1+\frac{R}{R_\text{l}}\right)} = \frac{R_\text{l}}{R+R_\text{l}}, \tag{32}$$

which indicates that the low-frequency response is only limited by the resistors R and R_l. On the other hand, at high frequencies

$$\lim_{\omega\to\infty} H_\text{c}(\omega) = \lim_{\omega\to\infty} \frac{1}{\omega^2LC} = 0, \tag{33}$$

which indicates that $H_\text{c}(\omega)$ has a low-pass characteristic.

A study of how each circuit element alters the pickup circuit frequency response is shown in Fig. 13, where a baseline pickup with $L = 2$ H, $R = 10\ \text{k}\Omega$, $C = 50$ pF, and $R_\text{l} = 1000\ \text{k}\Omega$ is considered, and each component is varied independently. A small variation in the DC resistance R, shown in Fig. 13(a), has little effect on the overall frequency response, affecting mostly the magnitude of the resonance peak at ω_R. Additionally, with the component values that were considered, $R_\text{l} \gg R$, the response at low frequencies is $H_\text{c}(0) \approx 1$ in Eq. (32).

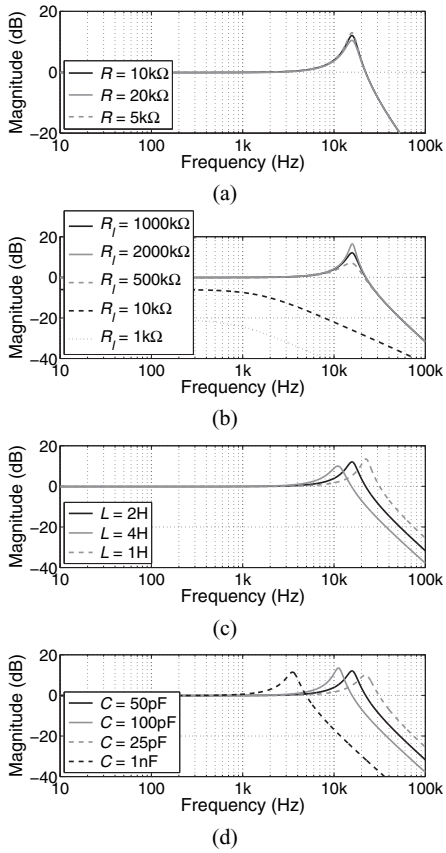

Fig. 13. Verification on the effect of variation of circuit elements on the magnitude response of the pickup circuit for a baseline pickup with $L = 2$ H, $R = 10\ \text{k}\Omega$, $R_\text{l} = 1000\ \text{k}\Omega$, and $C = 50$ pF with variation of (a) R, (b) R_l, (c) L, and (d) C.

The effect of the core loss resistor R_l in Fig. 13(b) is also shown to be small when small variations are considered. With $500\ \text{k}\Omega < R_\text{l} < 2000\ \text{k}\Omega$, the changes, compared to the reference case $R_\text{l} = 1000\ \text{k}\Omega$, are only on the damping of the resonant peak at ω_R, where large values of R_l are shown to make the resonance peak more pronounced.

In a typical connection for the guitar volume control, a parallel resistor is connected to the pickup output as in Fig. 14. As the volume control resistor is in parallel with the loss resistor R_l, the total resistance is smaller, thus affecting the magnitude at low frequencies as in Eq. (32). Additionally, in Fig. 13(b), extremely small values of R_l, namely $R_\text{l} = 1\ \text{k}\Omega$ and $R_\text{l} = 10\ \text{k}\Omega$, can be observed to not only reduce the

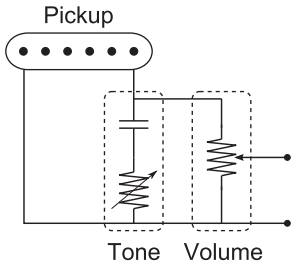

Fig. 14. Typical configuration of tone and volume control in electric guitars. Adapted from [24].

output level, but also damp the resonant peak. Hence, the volume control of a guitar also changes the coloration of the output signal.

The effect of the pickup inductance L is shown in Fig. 13(c). In this figure, L is shown to have an effect on the resonant frequency, since larger values of L push the resonance to lower frequency values. On the other hand, L also has an effect on the magnitude of the resonance peak. Additionally, by changing the resonant frequency ω_R, the energy at high frequencies is also changed since the low-pass decay starts at ω_R.

Just like the pickup inductor L, the output capacitance C shows a major effect on the pickup magnitude response in Fig. 13(d), which is also related to the resonant frequency ω_R and to the peak magnitude.

The tone control in a guitar connection is often implemented with a capacitance and a potentiometer, as shown in Fig. 14, which has the effect of increasing the equivalent output capacitance. As the typical value for the tone control capacitance is about 1 nF, Fig. 13(d) shows also the magnitude response with $C = 1$ nF. When the tone-control resistor is zero, the tone-control capacitor adds to C in Fig. 12(a), the resonance appears at a much lower frequency, and there is a significant decrease in the energy at high frequencies.

A practical measurement of the equivalent circuit is possible by analyzing the pickup impedance [24]. Additionally, a measurement setup is possible by using a second core with the magnetic field driven by a controlled external signal [24, 23, 44]. With this measurement setup it would be possible to determine the pickup transfer function, although the measurement will be also influenced by the impedance of the second core used in the measurement.

The digital model for this effect can be obtained in different manners. One approach is to obtain the discrete-time transfer function by applying the bilinear transform to Eq. (30) [4]. In this case, substituting $s = 2f_s(1 - z^{-1})/(1 + z^{-1})$ in Eq. (30) gives the discrete-time transfer function of the pickup circuit

$$H_c(z) = \frac{1 + 2z^{-1} + z^{-2}}{c_0 + c_1 z^{-1} + c_2 z^{-2}}, \tag{34}$$

where

$$c_0 = 1 + R/R_l + 2f_s L/R_l + 2f_s RC + 4f_s^2 LC \tag{35}$$

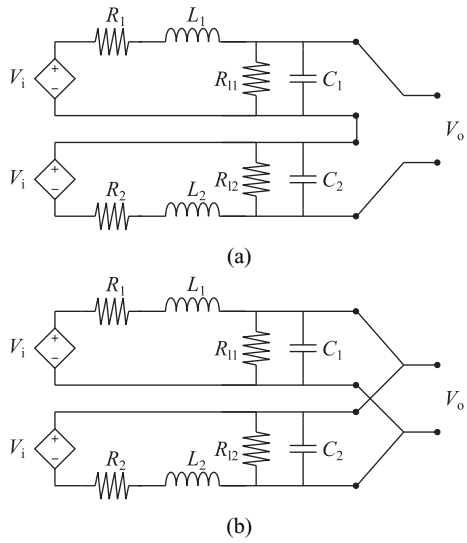

Fig. 15. Equivalent circuits for (a) series and (b) parallel connections of two pickups.

$$c_1 = 2 + 2R/R_l - 8f_s^2 LC \tag{36}$$

$$c_2 = 1 + R/R_l - 2f_s L/R_l - 2f_s RC + 4f_s^2 LC. \tag{37}$$

In another approach, a model using wave digital filters [45, 46] can be obtained. In this case, the magnetic behavior of the pickup permanent magnet can also be included as for power amplifier transformers [6]. In both approaches, note that when close to the Nyquist limit $f_s/2$, the resonance of the pickup f_R will be distorted due to the frequency warping caused by the bilinear transform.

5.1 Two Pickups in Parallel or in Series

The pickup combinations affect not only the guitar timbre through the phase differences, as shown in Section 2, but also the equivalent circuit. In addition to connecting two pickups in- or out-of-phase, the pickups may be connected in series or in parallel. This additional connection option not only varies the signal magnitude at the output jack but also affects the tone coloration.

Traditionally, the two coils on a humbucker pickup are connected in series to produce a loud "punchy" tone. The combination of two single-coil pickups (pickup selector positions 2 and 4 in a Stratocaster-style guitar) have traditionally been connected in parallel, resulting in a brighter tone while retaining the hum-canceling effect. Some guitars even offer the musician the choice of selecting the type of pickup connection (series/parallel and in-phase/out-of-phase) via electrical switches. The series and parallel pickup combinations are presented in Figs. 15(a) and (b), respectively, where pickups are modeled with circuit components L_x, C_x, R_x, and R_{lx}, where x is the pickup number.

If the sensed voltage in both pickups V_i is equal, which means that they are placed at the same position, the equivalent circuit for the parallel and series connection is obtained in order to evaluate the pickup combination effect. For both parallel and series connections, the equivalent circuits presented in Fig. 15 can be translated into the transfer function

$$H_{cc}(s) = \frac{a_0 + sa_1 + s^2 a_2}{b_0 + sb_1 + s^2 b_2 + s^3 b_3 + s^4 b_4}. \tag{38}$$

The transfer function coefficients for the series connection of Fig. 15(a) are

$$a_0 = 2R_{l1}R_{l2} + R_1 R_{l2} + R_{l1} R_2 \tag{39}$$

$$a_1 = R_{l1}(L_2 + R_2 R_{l2} C_2) + R_{l2}(L_1 + R_1 R_{l1} C_1) \tag{40}$$

$$a_2 = R_{l1}R_{l2}(L_1 C_1 + L_2 C_2) \tag{41}$$

$$b_0 = (R_1 + R_{l1})(R_2 + R_{l2}) \tag{42}$$

$$b_1 = (R_1 + R_{l1})(L_2 + R_2 R_{l2} C_2) + (R_2 + R_{l2})(L_1 + R_1 R_{l1} C_1) \tag{43}$$

$$b_2 = (R_1 + R_{l1}) R_{l2} L_2 C_2 + (R_2 + R_{l2}) R_{l1} L_1 C_1 + (L_1 + R_1 R_{l1} C_1)(L_2 + R_2 R_{l2} C_2) \tag{44}$$

$$b_3 = (L_1 + R_1 R_{l1} C_1) R_{l2} L_2 C_2 + (L_2 + R_2 R_{l2} C_2) R_{l1} L_1 C_1 \tag{45}$$

$$b_4 = R_{l1} R_{l2} L_1 L_2 C_1 C_2. \tag{46}$$

For the parallel connection of Fig. 15(b)

$$a_0 = R_1 + R_2 \tag{47}$$

$$a_1 = L_1 + L_2 \tag{48}$$

$$b_0 = R_1 R_2 \frac{R_{l1} + R_{l2}}{R_{l1} R_{l2}} + R_1 + R_2 \tag{49}$$

$$b_1 = L_1 + L_2 + R_1 R_2 (C_1 + C_2) + \frac{R_{l1} + R_{l2}}{R_{l1} R_{l2}} (R_1 L_2 + R_2 L_1) \tag{50}$$

$$b_2 = (R_1 L_2 + R_2 L_1)(C_1 + C_2) \frac{R_{l1} + R_{l2}}{R_{l1} R_{l2}} L_1 L_2 \tag{51}$$

$$b_3 = L_1 L_2 (C_1 + C_2) \tag{52}$$

$$a_2 = b_4 = 0. \tag{53}$$

When two pickups with the same equivalent circuit components are connected, the transfer function for the combined pickups can be simplified. In this case, a series connection would have the same transfer function as a single pickup, but with a gain of two, inductance $2L$, series resistance $2R$, core resistance $2R_l$, and capacitance $C/2$. The resulting transfer function

$$H_{cc}(s) = 2\frac{1}{\left(1 + \frac{R}{R_l}\right) + s\left(\frac{L}{R_l} + RC\right) + s^2 LC} \tag{54}$$

is the same as $H_c(s)$ in Eq. (30), but with a different gain. In the case of a parallel connection, no additional gain appears, and the equivalent components are inductance $L/2$, series resistance $R/2$, core resistance $R_l/2$, and capacitance $2C$, resulting in the same transfer function as $H_c(s)$ in Eq. (30).

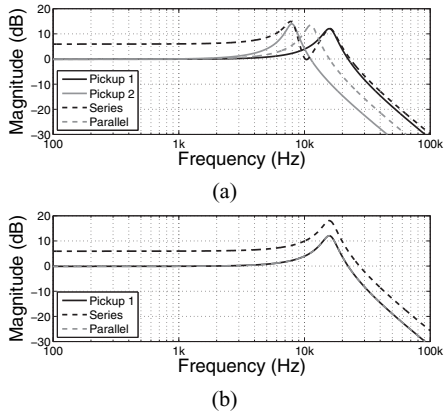

Fig. 16. Circuit frequency response for (a) a combination of two different pickups, and (b) a combination of identical pickups.

The frequency responses for various combinations of pickups are shown in Fig. 16. Two different pickups are considered in Fig. 16(a). Pickup 1 has the following equivalent components: $L_1 = 2$ H, $R_1 = 10$ kΩ, $C_1 = 50$ pF, and $R_{l1} = 1000$ kΩ. Pickup 2 is modeled with $L_2 = 4$ H, $R_2 = 20$ kΩ, $C_2 = 100$ pF, and $R_{l2} = 2000$ kΩ. In this case, pickups 1 and 2 have different resonant frequencies at $f_{R,\,1} = 16$ kHz and $f_{R,\,2} = 8$ kHz with a gain of 12 dB and 14 dB, respectively.

The result for two different pickups combined in series is shown in Fig. 16(a). In this case an increase of 6 dB is observed at low frequencies and two resonant peaks are present at the same frequencies as the ones observed in pickups 1 and 2. The behavior at higher frequencies is similar to the one observed for pickup 1, which has the highest resonant frequency $f_{R,\,1}$. At frequencies between the resonant peaks, a minimum is observed, with an attenuation of 6 dB in relation to the gain at low frequencies. It is interesting to notice that for the series combination of different pickups, the resonant peaks have an equivalent lower gain, since in most of the frequency range the gain is 6 dB, whereas at the resonant peak the gain reaches 15 dB, which indicates an increase of 9 dB.

When two different pickups are combined in parallel, as shown in Fig. 16(a), a single resonant peak is present in the frequency response, which is located at a frequency between the resonances of pickups 1 and 2. In this case,

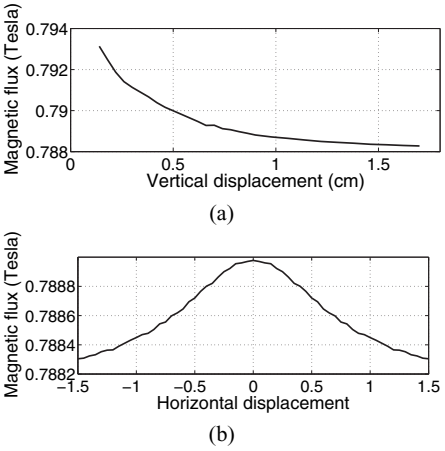

Fig. 17. Finite element simulation of a magnet and a string, where the magnetic flux density in Tesla was measured at the center of the magnet. The simulation result for (a) string displacement normal to the magnet face and (b) along the magnet face.

the behavior at low frequencies is not affected much, and the combined pickup resembles a single pickup with an intermediate resonant frequency.

The response for the combination of two identical pickups is shown in Fig. 16(b), with $L = 2$ H, $R = 10$ kΩ, $C = 50$ pF, and $R_l = 1000$ kΩ. A series combination of equal pickups is observed to provide the same frequency response with a gain of 6 dB. In the case of a parallel connection, the same frequency response is obtained as for the original pickups. Differences may be noticed in these cases when taking into account the interaction with the components connected to the pickup. Although no great difference is observed in the frequency response, as the equivalent output capacitance is lower for the series connection and higher for the parallel, the sensitivity to the components connected to the pickup will be changed. In the case of the series connection, the sensitivity to the impedance of the cables and other circuitry connected to the pickups will be increased, whereas the parallel connection will be more robust.

6 PICKUP NONLINEARITY

A pickup captures string motion by changes caused in the magnetic flux depending on the proximity of the string to the magnet [30]. Pickups are built using permanent magnets having fixed magnetizing force H, and as the string moves, the magnetic permeability μ is changed. This change in permeability is mapped into a change in the magnetic flux Φ, which is converted into an electrical voltage by the pickup winding. The mapping between the string position and the magnetic flux is nonlinear, which enhances the string harmonics. Both [25] and [26] describe methods to determine the pickup magnetic flux.

A finite element simulation using Vizimag [47] was performed for a theoretical pickup, with results shown in Fig. 17. The two-dimensional simulation was performed

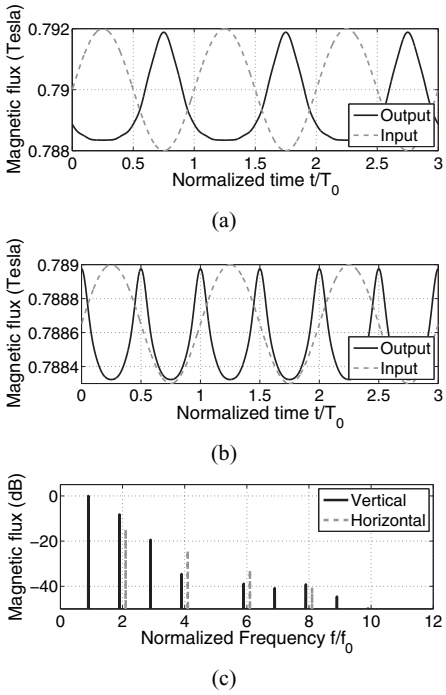

Fig. 18. Response for a sinusoidal signal with nonlinear interpolation of points in Fig. 17. (a) The time response for string displacement normal to the magnet face, (b) the time response for string displacement along the magnet face, and (c) the frequency response for both kinds of displacement. A small frequency offset is used in (c) to the make visualization of the vertical and horizontal spectra easier.

considering a rectangular magnet 17 mm x 5 mm, representing a cross section of the permanent magnet, and a disk of high permeability material with a 2-mm diameter, which represents the cross section cut of the string. The results in Fig. 17(a) show an exponential decay of the magnetic flux as the string moves away from the permanent magnet in the vertical direction. On the other hand, Fig. 17(b) shows a bell-shaped curve for horizontal displacements around the center of the magnet.

The nonlinear flux response for a sinusoidal string vibration is shown in Fig. 18, where a scaled version of the input signal is also presented to improve visualization. This example was generated by interpolating the nonlinear function described in Fig. 17. The response for displacement normal to the face of the magnet is shown in Fig. 18(a). Since the response for this kind of signal is asymmetric, the frequency content shown in Fig. 18(c) for vertical polarization reveals that both odd and even harmonics are generated, with a high emphasis up to the third harmonic.

On the other hand, the response for displacement parallel to the magnet face, shown in Fig. 18(b), has twice the frequency of the original signal. From Fig. 17(b) the horizontal vibrations are observed to be rectified by the pickup nonlinearity, since both the maximum and the minimum values of the input signal are mapped onto minimum

values in the output signal. The result of this effect is shown in Fig. 18(c), where only even harmonics are present for the horizontal polarization.

The results shown in Fig. 18 indicate that different polarization patterns in the string will have different coloration impacts. When more energy is present in the horizontal polarization, odd harmonics will be suppressed. Additionally, time-varying polarization of the string will lead to a varying harmonic pattern, with either more odd or even harmonics, which can enhance the guitar timbre.

7 CONCLUSION

This work has presented the properties of the physical phenomena and modeling techniques related to guitar pickups. The importance of modeling the pickup phenomena is related to proper synthesis of steel string instruments, such as the guitar or bass guitar, and emulation of different pickups in digital audio effects processing.

The pickup position was modeled by using a waveguide framework. With this approach it is possible to describe the frequency coloration with relation to the pickup position, as well as to design a digital filter that emulates it. A comparison of different pickup positions have explained why guitar pickups placed next to the bridge have a bright sound, while neck and middle positions have a darker sound. The pickup sensitivity width is explained and a novel model is proposed by using the same waveguide approach, which has shown that the pickup sensitivity has a low-pass effect on the output signal.

The results for the pickup position were used to determine the effect of mixing different pickup signals when identical pickups are used. It was shown that for some configurations with opposite pickup phase, the first harmonic was mostly suppressed. For configurations with in-phase mixing, a wider first lobe in the frequency response was observed, which enhances the response for the fundamental frequency over most of the string pitches. Additionally, the response when mixing pickup signals shows a more complex pattern, which depends on the difference and the average of the positions of the pickups. For pickups with different resonant frequencies, the mixing response will very likely differ significantly from that found in this work, since phase differences between pickup circuit responses will change the constructive and destructive interactions between frequencies.

The effect caused by non-ideal wave propagation in strings is analyzed by considering dispersion, or a frequency-dependent propagation speed. In the analysis performed, for the dispersive string behavior, the comb-filter effect caused by the pickup position was seen to have its maxima and notches at inharmonic positions. Two modeling approaches are presented, both including all-pass filters to emulate the frequency-dependent propagation speed of waves in stiff strings.

An analysis of the equivalent circuit elements was performed, where the influence of each element was observed individually. The inductance and capacitance in the model have been shown to have a major effect on the position of the resonance peak the pickups usually have in their transfer function. This resonance peak is responsible for the distinctive sound of each individual pickup. The DC resistance has little effect on the pickup transfer function but has some effect on the damping of the resonance peak. The core loss resistance is seen to influence the amplitude of the resonance peak. Additionally, typical volume control circuits for guitar were shown to interact with this resistance, and at extreme values a damping of the pickup resonance was observed.

The nonlinear behavior of the pickup was demonstrated using a finite element simulation. The results show that the polarization of the string movement affects the output timbre by adding more even harmonic content for high energy in horizontal polarization, or odd harmonic content for vertical polarization.

The results and new models presented here can be used both in musical sound synthesis and in the implementation of digital effects. Since most of the models are string dependent, their application to synthesis models is straightforward, since they often use a waveguide approach. For the implementation of audio effects for real guitar signals, non-magnetic hexaphonic pickups (such as piezoelectric ones) separating the signal streams for each string would be needed. Several commercial implementations of such pickup systems currently exist.

8 ACKNOWLEDGMENTS

This research was funded by CIMO, Aalto University, and Academy of Finland (project 122815). The authors also thank Julian Parker and Luis Costa de Jussilainen for their helpful comments.

REFERENCES

[1] A. Case, "Recording Electric Guitar – The Science and the Myth," *J. Audio Eng. Soc.*, vol. 58, no. 1/2, pp. 80–83 (2010 Jan./Feb.).

[2] T. D. Rossing, R. F. Moore, and P. A. Wheeler, *The Science of Sound*, 3rd ed. (Addison-Wesley, 2002).

[3] S. Bilbao and M. Rath, "Time Domain Emulation of the Clavinet," presented at the *128th Convention of the Audio Engineering Society*, (2010 May), convention paper 8014.

[4] V. Välimäki, S. Bilbao, J. O. Smith, J. S. Abel, J. Pakarinen, and D. Berners, "Virtual Analog Effects," in *DAFX - Digital Audio Effects*, 2nd ed., U. Zölzer, Ed. (John Wiley & Sons, 2011), ch. 12, pp. 473–522.

[5] D. Yeh, J. Abel, and J. Smith, "Automated Physical Modeling of Nonlinear Audio Circuits for Real-Time Audio Effects – Part I: Theoretical Development," *IEEE Trans. Audio, Speech, and Language Processing*, vol. 18, no. 4, pp. 728–737 (May 2010).

[6] R. C. D. Paiva, J. Pakarinen, V. Välimäki, and M. Tikander, "Real-Time Audio Transformer Emulation for Virtual Tube Amplifiers," *EURASIP Journal on Advances in Signal Processing*, vol. 2011, pp. 1–15 (2011).

[7] J. Pakarinen and M. Karjalainen, "Enhanced Wave Digital Triode Model for Real-Time Tube Amplifier Emulation," *IEEE Trans. Audio, Speech, and Language Processing*, vol. 18, no. 4, pp. 738–746 (2010).

[8] K. Dempwolf, M. Holters, and U. Zölzer, "Discretization of Parametric Analog Circuits for Real-Time Simulations," in *Proc. of the DAFx'10, 13th International Conference on Digital Audio Effects*, Graz, Austria, September 2010, pp. 1–8.

[9] V. Välimäki, J. D. Parker, and J. S. Abel, "Parametric Spring Reverberation Effect," *J. Audio Eng. Soc.*, vol. 58, no. 7/8, pp. 547–562 (2010 July).

[10] V. Välimäki, J. D. Parker, L. Savioja, J. O. Smith, and J. S. Abel, "Fifty Years of Artificial Reverberation," *IEEE Trans. Audio, Speech, and Language Processing*, vol. 20, no. 5, pp. 1421–1448 (July 2012).

[11] C. Gough, "Electric Guitar and Violin," in *The Science of String Instruments*, 1st ed., T. D. Rossing, Ed. (Springer, 2010), ch. 22, pp. 393–415.

[12] J. O. Smith, "Physical Modeling Using Digital Waveguides," *Computer Music Journal*, vol. 16, no. 4, pp. 74–91 (1992).

[13] C. R. Sullivan, "Extending the Karplus-Strong Algorithm to Synthesize Electric Guitar Timbres with Distortion and Feedback," *Computer Music Journal*, vol. 14, no. 3, pp. 26–37 (1990).

[14] M. Karjalainen, V. Välimäki, and T. Tolonen, "Plucked-String Models: From the Karplus-Strong Algorithm to Digital Waveguides and Beyond," *Computer Music Journal*, vol. 22, no. 3, pp. 17–32 (1998).

[15] P. Cook, "Computer Music," in *Springer Handbook of Acoustics*, T. D. Rossing, Ed. (Springer, 2001), ch. 17, pp. 713–742.

[16] V. Välimäki, J. Huopaniemi, M. Karjalainen, and Z. Jánosy, "Physical Modeling of Plucked String Instruments with Application to Real-Time Sound Synthesis," *J. Audio Eng. Soc.*, vol. 44, no. 5, pp. 331–353 (1996 May).

[17] G. Evangelista and F. Eckerholm, "Player-Instrument Interaction Models for Digital Waveguide Synthesis of Guitar: Touch and Collisions," *IEEE Trans. Audio, Speech, and Language Processing*, vol. 18, no. 4, pp. 822–832 (May 2010).

[18] N. Lee and J. O. Smith, "Virtual String Synthesis," in *The Science of String Instruments*, 1st ed., T. D. Rossing, Ed. (Springer, 2010), ch. 23, pp. 417–455.

[19] S.-J. Cho, U.-P. Chong, and S.-B. Cho, "Synthesis of the Dan Trahn Based on a Parameter Extraction System," *J. Audio Eng. Soc.*, vol. 58, no. 6, pp. 498–507 (2010 June).

[20] A. Hoshiai, "Musical Tone Signal Forming Device for a Stringed Musical Instrument," *US Patent* 5,367,120, Nov. 22, 1994.

[21] ——, "Musical Tone Signal Forming Apparatus for Use in Simulating a Tone of String Instrument," *US Patent* 5,731,533, March 24, 1998.

[22] J. D. Tillman. (2000, July) Response Effects of Guitar Pickup Mixing. (visited in February 24, 2012). [Online]. Available: http://www.till.com/articles/PickupMixing/index.html

[23] M. Koch, *Building Electric Guitars* (Nürtingen, Germany: Koch Verlag, 2001).

[24] T. Jungmann, "Theoretical and Practical Studies on the Behavior of Electric Guitar Pickups," Master's thesis, Department of Electrical Engineering, Acoustics Laboratory, Helsinki University of Technology, Espoo, Finland, 1994. [Online]. Available: http://www.acoustics.hut.fi/publications/files/theses/jungmann_mst.pdf

[25] N. G. Horton and T. R. Moore, "Modeling the Magnetic Pickup of an Electric Guitar," *American Journal of Physics*, vol. 77, no. 2, pp. 144–150 (February 2009).

[26] G. Lemarquand and V. Lemarquand, "Calculation Method of Permanent-Magnet Pickups for Electric Guitars," *IEEE Trans. Magnetics*, vol. 43, no. 9, pp. 3573–3578 (September 2007).

[27] M. Karjalainen, T. Mäki-Patola, A. Kanerva, and A. Huovilainen, "Virtual Air Guitar," *J. Audio Eng. Soc.*, vol. 54, no. 10, pp. 964–980 (2006 October).

[28] F. Eckerholm and G. Evangelista, "The PluckSynth Touch String," in *Proc. of the DAFx'08- 11th International Conference on Digital Audio Effects*, Espoo, Finland, Sept. 2008, pp. 213–220.

[29] N. Lindroos, H. Penttinen, and V. Välimäki, "Parametric Electric Guitar Synthesis," *Computer Music Journal*, vol. 35, no. 3, pp. 18–27 (September 2011).

[30] T. D. Rossing and G. Caldersmith, "Guitars and Lutes," in *The Science of String Instruments*, 1st ed., T. D. Rossing, Ed. (Springer, 2010), ch. 3, pp. 19–46.

[31] J. D. Tillman. (2002, October) Response Effects of Guitar Pickup Position and Width. (visited in February 24, 2012). [Online]. Available: http://www.till.com/articles/PickupResponse/index.html

[32] T. I. Laakso, V. Välimäki, M. Karjalainen, and U. K. Laine, "Splitting the Unit Delay – Tools for Fractional Delay Filter Design," *IEEE Signal Processing Magazine*, vol. 13, no. 1, pp. 30–60 (January 1996).

[33] H. Järveläinen and M. Karjalainen, "Perceptibility of Inharmonicity in the Acoustic Guitar," *Acta Acustica united with Acustica*, vol. 92, no. 5, pp. 842–847 (October 2006).

[34] N. H. Fletcher and T. D. Rossing, *The Physics of Musical Instruments* (Springer-Verlag, 1998).

[35] J. Rauhala and V. Välimäki, "Tunable Dispersion Filter Design for Piano Synthesis," *IEEE Signal Processing Letters*, vol. 13, no. 5, pp. 253–256 (May 2006).

[36] J. Rauhala, "Physics-Based Parametric Synthesis of Inharmonic Piano Tones," Ph.D. dissertation, Helsinki University of Technology, Espoo, Finland, 2007. [Online]. Available: http://lib.tkk.fi/Diss/2007/isbn9789512290666/

[37] S. A. Van Duyne and J. O. Smith, "A Simplified Approach to Modeling Dispersion Caused by Stiffness in Strings and Plates," in *Proc. of the ICMC'94, International Computer Music Conference*, vol. 1, Denmark, September 1994, pp. 407–410.

[38] I. Testa, G. Evangelista, and S. Cavaliere, "Physically Inspired Models for the Synthesis of Stiff Strings with Dispersive Waveguides," *EURASIP Journal on*

Applied Signal Processing, vol. 2004, no. 7, pp. 964–977 (2004).

[39] J. S. Abel, V. Välimäki, and J. O. Smith, "Robust, Efficient Design of Allpass Filters for Dispersive String Sound Synthesis," *IEEE Signal Processing Letters*, vol. 17, no. 4, pp. 406–409 (April 2010).

[40] J. Pakarinen, M. Karjalainen, V. Välimäki, and S. Bilbao, "Energy Behavior in Time-Varying Fractional Delay Filters for Physical Modeling Synthesis of Musical Instruments," in *Proc. of the IEEE International Conference on Acoustics, Speech, and Signal Processing 2005*, vol. 3, Philadelphia, USA, March 2005, pp. 1–4.

[41] A. Härmä, M. Karjalainen, L. Savioja, V. Välimäki, U. K. Laine, and J. Huopaniemi, "Frequency-Warped Signal Processing for Audio Applications," *J. Audio Eng. Soc.*, vol. 48, no. 11, pp. 1011–1031 (2000 Nov).

[42] A. Härmä, "Frequency-Warped Autoregressive Modeling and Filtering," Ph.D. dissertation, Helsinki University of Technology, Espoo, Finland, 2001. [Online]. Available: http://lib.tkk.fi/Diss/2001/isbn9512254603/

[43] V. Välimäki, J. S. Abel, and J. O. Smith, "Spectral Delay Filters," *J. Audio Eng. Soc.*, vol. 57, no. 7/8, pp. 521–531 (2009 July/Aug).

[44] H. E. W. Lemme. (2009, February) The Secrets of Electric Guitar Pickups. (visited in December 10, 2010). [Online]. Available: http://buildyourguitar.com/resources/lemme/

[45] A. Fettweis, "Wave Digital Filters: Theory and Practice," *Proc. of the IEEE*, vol. 74, no. 2, pp. 270–327 (February 1986).

[46] V. Välimäki, J. Pakarinen, C. Erkut, and M. Karjalainen, "Discrete-Time Modelling of Musical Instruments," *Reports on Progress in Physics*, vol. 69, no. 1, pp. 1–78 (January 2006).

[47] J. S. Beeteson. Vizimag: Visualizing Magnetic Fields. [Online]. Available: http://www.vizimag.com/

THE AUTHORS

Rafael Cauduro Dias de Paiva

Jyri Pakarinen

Vesa Välimäki

Rafael Cauduro Dias de Paiva is a doctoral student at the Aalto University School of Electrical Engineering, Espoo, Finland, since 2010 and is a researcher at Nokia Institute of Technology (INdT), Brasilia, Brazil, since 2008. Rafael Paiva obtained his Bachelor's degree in electrical engineering from the Federal University of Santa Maria (UFSM) in 2005, and the Master's degree in signal processing from the Federal University of Rio de Janeiro (UFRJ) in 2008. Paiva has been involved with audio signal processing since 2006, when he conducted research on voice/speech pitch modification and morphing. His ongoing doctoral research focuses on real-time models of nonlinear analog audio systems, which includes models for guitar amplifiers and other guitar related phenomena. At INdT, Rafael Paiva develops simulation tools and new solutions for wireless networks for standardization forums. Among his research interests are real-time models for vintage nonlinear analog effects and vacuum tube amplifiers; audio and speech synthesis, effects and coding; new technologies; and standardization of wireless networks.

●

Jyri Pakarinen was born in Lappeenranta, Finland, in 1979. He received the M.S. and D.S. (tech.) degrees in acoustics and audio signal processing from the Helsinki University of Technology in 2004 and 2008, respectively. Dr. Pakarinen worked as a researcher in the Aalto University, Finland, from 2002 until 2011. His research work focused on sound synthesis through physical modeling, digital emulation of electric audio circuits, and vibroacoustical measurements. He was the Lead Guest Editor of a special issue of the *EURASIP Journal on Advances in Signal Processing* in 2011. Dr. Pakarinen is currently working for Dolby Sweden AB in Stockholm, Sweden.

●

Vesa Välimäki is professor of audio signal processing at the Aalto University, Espoo, Finland. He received his M.Sc. in Technology, Licentiate of Science in Technology, and Doctor of Science in Technology degrees in electrical engineering from the Helsinki University of Technology (TKK) in 1992, 1994, and 1995, respectively. His doctoral dissertation dealt with fractional delay filters and physical modeling of musical wind instruments.

In 1996 he was a postdoctoral research fellow at the University of Westminster, London, UK. In 2001–2002 he was professor of signal processing at the Pori School of Technology and Economics, Tampere University of Technology, Pori, Finland. In 2006–2007, he was the Head of the TKK Laboratory of Acoustics and Audio Signal Processing. During the academic year 2008–2009 he was a visiting scholar at the Center for Computer Research in Music and Acoustics (CCRMA), Stanford University, Stanford, CA. His research interests include sound synthesis, audio effects processing, digital filter design, and acoustics of musical instruments.

Prof. Välimäki is a fellow of the Audio Engineering Society, a senior member of the IEEE Signal Processing Society, a life member of the Acoustical Society of Finland, and a member of the Finnish Musicological Society. He was the papers chair of the AES 22nd International Conference on Virtual, Synthetic, and Entertainment Audio in 2002. He was the chairman of the 11th International Conference on Digital Audio Effects (DAFx-08), which was held in Espoo, Finland, in 2008.